Non-linear astrochemical kinetics: theory and applications

Dufour, G.C.

4 Oscillations in Gas-grain Astrochemical Kinetics

Abstract

We have studied gas-grain chemical models of interstellar clouds to search for nonlinear dynamical evolution. A prescription is given for producing oscillatory solutions when a bistable solution exists in the gas-phase chemistry and we demonstrate the existence of limit cycle and relaxation oscillations solutions in astrochemistry. As the autocatalytic chemical processes underlying these solutions are common to all models of interstellar chemistry, the occurrence of these solutions should be widespread. We briefly discuss the implications for interpreting molecular cloud composition with time-dependent models and some future directions for this approach.

Dufour, G., Charnley, S. B. & Lindberg, J. 2022, "Oscillations in Gas-grain Astrochemical Kinetics" In *Mon. Not. Astron. Soc., submitted*

4.1 Introduction

The systems of differential equations governing the kinetics of chemical reaction networks can exhibit a wide range of nonlinear dynamical phenomena: limit cycles, complex oscillations and chaos can all emerge from stable stationary solutions, subject to variation of externally-controlled bifurcation parameters (Gray & Scott (1996); Scott (1991)). One signpost of possible non-linear chemical kinetics is the presence of bistability in the stationary, steady-state, solutions (i.e. the fixed points) of the associated system of differential equations. In chemical systems, multistability can arise when autocatalysis is present, i.e. when one species, the autocatalyst, can take part in reaction sequences which promote its formation. When the stationary solutions become unstable a Hopf bifurcation emerges and limit cycle oscillations can occur.

In the simplest, purely gas-phase, chemical models of dense interstellar clouds, the chemistry is driven by cosmic-ray ionization of H_2 and evolves to approach a steady-state on time-scales of typically $\sim$ few $\times 10^6$ years. In all cases the chemistry tends to follow well-defined evolutionary pathways and, when making comparisons with observed molecular abundances, it has become common to label this as 'late-time' chemistry, whereas so-called 'early-time' chemistry occurs around $\sim$ few $\times 10^5$ years (Leung et al. (1984)). The accretion and desorption of atomic and molecular material onto and from dust grains leads to the formation of molecular ice mantles. When desorption is inefficient, species can be completely lost from the gas (e.g. Leung et al. (1984)); when desorption mechanisms can compete with accretion a quasi-steady-state can persist (e.g. Willacy & Williams (1993); Willacy & Millar (1998); Charnley et al. (2001)). This occurs a time-scale determined by the gas density, the grain-size distribution and the dust physics, but is typically comparable to, or longer than, that for 'early-time' chemistry and shorter than that for 'late-time' chemistry. Hence, the possibility of that oscillatory and chaotic solutions could manifest themselves would have major implications for modeling and interstellar clouds, and astrochemistry in general.

The existence of bistable solutions in interstellar gas-phase chemistry has been recognized for some time (Pineau des Forets et al. (1992); Le Bourlot et al. (1993)) and has been the subject of several studies (e.g. Le Bourlot et al. (1995a,b); Lee et al. (1998); Pineau Des Forêts & Roueff (2000); Viti et al. (2001); Charnley & Markwick (2003); Wakelam et al. (2006b)). This raises the prospect that oscillations and chaos could be common but heretofore unrealized solutions to well-studied chemical models. However, it is only recently that limit cycle oscillations have been reported.[1] Roueff & Le Bourlot (2020) showed that sustained chemical oscillations, could occur in purely gas-phase models of dense molecular clouds. They found that the oscillations originated in the nitrogen chemistry for temperatures in the range $T \approx 7 - 15$K and was controlled by the H_2 ortho/para ratio. Roueff & Le Bourlot presented an

[1] Le Bourlot et al. (1993) did previously report one case of limit cycle oscillations in a gas-phase dense cloud model.

overview of the important chemical reactions in their model, identifying deuterium chemistry as an important component, but no underlying mechanism, such as emergence from a bistable state, was identified.

Dufour & Charnley (2019) (Paper I) demonstrated that the known astrochemical bistable solutions have an autocatalytic origin in oxygen chemistry. Dufour & Charnley (2021) (Paper I & II) further showed that autocatalysis and bistability can also occur in the nitrogen and carbon chemistry. of dense molecular clouds. In each case, autocatalysis involves dimer-autocatalyst pairs: O_2-O, N_2-N, CH-C_2H_2, with other autocatalytic cycles also being possible in carbon chemistry (e.g. C_2). It is known that limit cycle oscillations can be induced in a bistable chemical system in which species crucial to autocatalysis are removed and re-introduced by an additional feedback process which occurs on a time-scale longer or comparable to that of the chemical reactions, i.e. the feedback renders the stationary solutions unstable (e.g. Sagués & Epstein (2003)). In interstellar clouds, the exchange of atoms and molecules between gas and dust grains naturally provides this process.

The plan of this article is as follows. In section 4.2 we summarize the mathematical structure of the model with respect to bistable gas-phase solutions and the gas-grain interaction. The parameters adopted in a reference chemical model are presented in section 4.3. In section 4.4 we show that introducing accretion and desorption of atomic and molecular oxygen into a simple reduced model of interstellar chemistry, with known autocatalytic pathways and bistable solutions, leads to chemical oscillations. We then show that oscillatory solutions are also present in more realistic models of dense cloud chemical evolution (section 4.5). Extension of the modeling are briefly discussed in section 4.6 and conclusions are given in section 4.7.

4.2 Theory

4.2.1 Bistable solutions in gas-phase chemistry

The chemical evolution of N gas-phase chemical species in static dense molecular gas is obtained by solving the system of autonomous nonlinear ordinary differential equations (ODEs)

$$\dot{y}_i = G_i = n_{\rm H}\Big[\sum_j \sum_m k_{jm} y_j y_m - y_i \sum_s k_{is} y_s\Big] + \sum_u \beta_u y_u - y_i \sum_w \beta_w; \qquad i = 1, ..., N \quad (4.1)$$

where $n_{\rm H}$ is the density of hydrogen nuclei ($n_{\rm H}(= n({\rm H}) + 2{\rm n}({\rm H}_2)$; fractional abundance of species i, $y_i(t)$, is equal to $n_i/n_{\rm H}$, for number density n_i; and k_{jm}, β_u, β_w are reaction rate coefficients for various bimolecular and unimolecular processes. This system is solved subject to prescribed values of the cosmic ray ionization rate ζ, the hydrogen

nucleon number density $n_{\rm H}$, the gas temperature T, the visual extinction, A_V, and the total elemental abundances, $Y_j^{\rm T}$, of the major volatile elements and the refractory metals (e.g. j=C,O,N,S,Si,Na), The elemental abundances are defined relative to a reference value, values of X_j (e.g. a diffuse cloud line of sight) and a depletion factor, δ_j, as $Y_j^{\rm T} = X_j\delta_j$; we used the same values of X_j as in papers I and II. The reaction rate coefficients are assumed to remain constant in time. For a defined set of initial conditions on the N species, $y_i(0)$, the time-dependent solution can be obtained with a stiff ODE solver such as DVODE (Nejad (2005)).

It is necessary to examine the steady-state solutions for bistability and other bifurcation phenomena. The system of differential equation can only yield stable solutions and so, as both the stable and unstable solutions are necessary to fully characterize the bifurcations, we require to use Newton-Raphson iteration to solve the system

$$G_i(\mathbf{y}; \zeta/n_{\rm H}, \zeta_{\rm He}, T, A_V, \beta_{\rm crp}, Y_C^{\rm T}, Y_O^{\rm T}, Y_N^{\rm T}, Y_S^{\rm T}, Y_{Na}^{\rm T}) = 0 \qquad i = 1, ..., N. \quad (4.2)$$

The appearance/disappearance of bistable solutions is principally controlled by variation of the bifurcation parameters: the cosmic-ray ionization of H_2 and He, through the ratios $\zeta/n_{\rm H}$ and $\zeta_{\rm He}/n_{\rm H}$, the presence of cosmic ray-induced photons $\beta_{\rm crp}$, the relative elemental depletions $Y_j^{\rm T}$, and the H_3^+ electron recombination rate, α_3 (Le Bourlot et al. (1993, 1995a); Lee et al. (1998); Pineau Des Forêts & Roueff (2000); Wakelam et al. (2006b); Dufour & Charnley (2019, 2021)).

4.2.2 Gas-grain interaction in cold interstellar clouds

For each neutral species i, the coupled evolution of gas and grain-surface abundances is described by the differential equations

$$\dot{y}_i = G_i - \lambda_i y_i + \xi_i g_i \quad (4.3)$$

$$\dot{g}_i = \lambda_i y_i - \xi_i g_i \quad (4.4)$$

where g_i is the fractional abundance of i currently resident on dust. Sticking collisions of gaseous species with dust occur at the accretion rate, λ_i, and surface species leave the dust grain at the desorption rate, ξ_i (e.g. Brown & Charnley (1990)). These differential equations satisfactorily account for the exchange of material between the gas and dust and, as we show, are sufficient to investigate the effects of dust on bistable solutions without attempting to explicitly consider grain-surface chemical reactions (see §4.2.2). The effect of dust on bifurcations is that, on time-scales longer than the gas particle accretion accretion time ($\sim 1/\lambda_i$), the elemental abundances in the gas, Y_j, are set by the desorption rate of particles containing element j, and so we can expect $Y_j < Y_j^{\rm T}$. Thus, for each pair of species involved in an autocatalytic cycle, X and X_2, the ratios $\lambda_{\rm X}/\xi_{\rm X}$ and $\lambda_{\rm X_2}/\xi_{\rm X_2}$ will be bifurcation parameters. We model the gas-grain interaction as follows.

Accretion

Neutral atoms and molecules collide and stick to a distribution of dust grains at an accretion rate given by

$$\lambda_i = (\frac{8kT}{\pi M_i m_{\rm H}})^{1/2} S_i < n_{\rm gr}(a)\sigma(a) > \tag{4.5}$$

where k is the Boltzmann constant, M_i is the molecular weight (in a.m.u), S_i is the sticking efficiency, $n_{\rm gr}(a)$ is the number density of grains of radius a, and $\sigma(a)$ the grain collision cross-section. Assuming a single-size distribution of spherical grains with $a = 0.1$, $n_{\rm gr}(a) = 10^{-12} n_{\rm H}$, and $S_i = 1$ for neutral species heavier than He, one has

$$\lambda_i = 1.45 \times 10^4 D_{\rm gr} (\frac{T}{M_i})^{1/2} n_{\rm H} \tag{4.6}$$

where $D_{\rm gr}$ is the total available dust cross-section

$$D_{\rm gr} = \frac{< n_{\rm gr}(a)\sigma(a) >}{n_{\rm H}} \tag{4.7}$$

In dense clouds, electron sticking leads to negatively-charged grains dominating the dust distribution (Umebayashi & Nakano (1990)). We assume that when atomic ions collide with grains they are neutralized and released into the gas. Molecular ions will not be affected by grain interaction as electron recombination is more efficient at the densities of interest. As shown in Paper I, only grain neutralization of H^+ and S^+ can affect bistable solutions. However, the total grain-surface cross-section and elemental S abundance both to have values that are far larger than those inferred for dense molecular clouds (see Table 1). The values adopted here exclude the possibility of ion-grain neutralization affecting the occurrence of bistable solutions.

Desorption

We adopt simple thermal desorption as the mechanism for returning volatile atoms and molecules to the gas. A neutral molecule i thermally desorbs at a rate

$$\xi_i \; = \; \nu_i \exp[-\frac{E_i}{kT_{\rm gr}}] \tag{4.8}$$

where $T_{\rm gr}$ is the grain temperature, $\nu_i = 10^{12}$ s^{-1} is the vibrational frequency of i in a surface binding site and E_i is its binding energy for physisorption. With the E_i defined, the exponential dependence on $T_{\rm gr}$ means that it largely determines the gas-dust bifurcation parameters for each autocatalyst-dimer pair, $X - X_2$, i.e. $\lambda_k/\xi_k, k = O, O_2$.

Thermal desorption is actually the most restrictive choice for this mechanism. ISM thermal physics in dark clouds predicts $T \approx T_{\rm gr}$, thus affecting λ_i through the

$T^{1/2}$ dependence, nonlinearly coupling the desorption and accretion rates, and the bifurcations. This coupling does not occur for nonthermal desorption rates, $\xi_{\rm NT}$. We briefly discuss other possible desorption mechanisms in §4.6.

Grain-surface reactions

Assuming that all accreted reactive species are instantaneously hydrogenated (e.g. C, CH, CH_2, and CH_3 become CH_4; N, NH, and NH_2 become NH_3; O and OH become H_2O; S and HS become H_2S, (e.g. Brown & Charnley 1990) means that no desorption can occur and that there will be no nonlinear feedback. As the gas-dust exchange of particles is accounted for by equations (4.3) and (4.4), the simplest approach is to neglect surface reactions. Our neglect of surface hydrogenation in particular will be justified *a posteriori* as we find that nonlinear kinetic effects become important when $T_{\rm gr} \approx 15$K and so H atom thermal desorption can be expected to suppress surface hydrogenation reactions ($E_{\rm B} \approx 600$K). We return to this issue in §4.6.

4.3 Chemical model

Table 4.1 lists the physical parameters of the reference dense cloud model. We employ the same gas-phase chemical reaction network as in Paper II. The reactions are taken from the UMIST 2012 database (McElroy et al. (2013)) and consists for 2001 reactions involving 136 chemical species containing H, He, C, O, N, S, Na, and Si atoms. Only photoprocesses resulting from cosmic-ray-induced photons are considered (Prasad & Tarafdar (1983)). We only consider a single value for the H_3^+ recombination rate α_3 (cf. Paper I). The chemical evolution is solved by integrating the system of differential equations in §4.2.1 with all species initially present as atoms, except for H_2.

4.3.1 Surface binding energies

For consistency, we have adopted the binding energies, $E_{\rm B}$, listed in the UMIST database (McElroy et al. (2013)) for this initial study. Alternative compilations exist (e.g. Penteado et al. (2017)) but we take the UMIST values as a reference for comparison with future studies. The binding energies of helium atoms and H_2 molecules are so small that they do not stick to grains even at at the low temperatures of our models. For atomic C, O and N we have taken the single value $E_{\rm B} = 800$K, based on simple polarizability arguments (Tielens & Allamandola (1987)), and so there is no difference in the desorption rates of these species that could complicate the analysis.

The UMIST $E_{\rm B}$ values are consistent with recent calculations and experiments for O_2, CO, N and N_2 (Penteado et al. (2017); Wakelam et al. (2017a); Ferrero et al. (2020); Molpeceres et al. (2020)) but recent work indicates differences in the binding energies of C and O atoms. The influence of O atom binding energies on the models

Table 4.1: Gas-grain Chemical Model Parameters

Hydrogen number density (cm^{-3})	n_H	1.0×10^4; 1.0×10^5
Cosmic ray ionization rate (s^{-1})	ζ_0	1.3×10^{-17}
Dust temperature (K)	T_{gr}	see text
Visual extinction (mag.)	A_V	10
H_3^+ electron recombination rate ($cm^3\ s^{-1}$)†	α_3	$6.7 \times 10^{-8} T_3^{-0.52}$
Total dust cross-section (cm^2)	D_{gr}^0	$10^{-22}\pi$
Gas temperature (K)	T	T_{gr}
Total elemental abundances:	Y_{He}^T	0.14
	Y_O^T	1.6×10^{-4}
	Y_C^T	6.0×10^{-5}
	Y_N^T	2.0×10^{-5}
	Y_S^T	2.0×10^{-8}
	Y_{Si}^T	0
	Y_{Na}^T	2.0×10^{-9}
Surface binding energies (K)‡:		
	E_O	800K
	E_N	800K
	E_C	800K
	E_S	1100K
	E_{O_2}	1000K
	E_{N_2}	790K
	E_{CO}	1150K

† $T_3 = T/300$K

‡ For the most volatile species; see McElroy et al. (2013) for others.

are discussed in §4.6. For C atoms, calculations by Shimonishi et al. (2018) indicate that they bind to water by chemisorption with $E_B \sim 16000$K. Our results should not be particularly sensitive to the atomic C thermal desorption rate since the chemical evolution of interest in our models only begins at around the gas-grain accretion timescale, at which point most of the initially abundant atomic C has already been incorporated into CO (after $\sim$ few $\times 10^5$ years).

4.4 Bifurcations and oscillations in interstellar oxygen chemistry

We first consider a simple reduced model, containing only hydrogen, helium and oxygen, that was previously studied in Papers I & II. This model has two possible autocatalytic pathways in the O-O_2 chemistry and is useful for understanding the network kinetics before considering larger, more realistic, chemical models. In the first instance, for this model and those considered later, we are primarily interested in the nonlinear dynamical evolution of the system of ODEs. We therefore integrate over time-scales much longer than either the estimated lifetime of molecular clouds (Kennicutt & Evans (2012)) or the time-scale to reach a gas-phase chemical steady-state (in the absence of accretion onto dust) to ensure that any instabilities which may develop in the long term are found.

For the model parameters of Table 1, we compute the bifurcation diagram as a function of n_H for different values of T_{gr}. We find that that oscillating solutions can exist in a limited range $T_{gr} \approx 14.5 - 15$K. Figure 4.1(a) shows the bifurcation diagram for the case of $T_{gr} = 14.70$K. The bistable stationary states at low n_H involve a *fold* bifurcation as found in earlier studies. It is due entirely to gas-phase chemistry and is set by ζ/n_H (Lee et al. (1998)) and Y_O^T; depletion of species onto dust is negligible and so the abundance of O nuclei in the gas, Y_O, approximately equals Y_O^T. From Paper II, neglecting dust, as Y_O^T is reduced this bifurcation moves to higher densities. Inclusion of the gas-dust exchange of species leads to Y_O being set by accretion-desorption of oxygen atoms and molecules and the emergence of two *Hopf* bifurcations, where the system transitions from stationary to periodic solutions. The Hopf points H_1 and H_2, cover the interval $7 \times 10^2 \lesssim n_H \lesssim 2{\times}10^4$ cm^{-3}, and $Y_O \ll Y_O^T$.

We were unable to fully characterize the Hopf bifurcations using Newton-Raphson iteration due to problems with branching and continuation to obtain the unstable solutions. The periodic solutions shown are those obtained with the ODE solver when carried out to 10^8 years. This approach was based on the premise that if stable periodic (limit cycle) oscillations emerge they will still be present on this time-scale and the amplitude maxima and minima for each species, y_{max} and y_{min}, should be constant; the solutions presented thus plot these (y_{max}, y_{min}) pairs at each n_H.

The Hopf bifurcations in Figure 4.1(a) can be classified as follows (Seydel (2009)). H_1 is a supercritical Hopf bifurcation. Periodic solutions are present in the immediate vicinity of H_1 where there is a *soft* transition from the stationary state. H_1 has a

pitchfork structure with an unstable stationary state connecting it to H_2 (not shown). H_2 is a subcritical Hopf bifurcation where, in this case, the periodic solutions occur after a jump from the stationary state, i.e. a *hard* transition. H_2 is connected to the two adjacent stable periodic solutions by two unstable periodic solutions (not shown).

Figure 4.1(b) shows the time series for the oscillatory solutions for $y_{\rm O}(t)$, $y_{\rm OH}(t)$ and $y_{\rm O_2}(t)$ at $n_{\rm H} = 1 \times 10^4$ cm^{-3}. These are limit cycle oscillation confirmed in the phase plane evolution as shown in Figure 4.1(c).

4.5 Relaxation oscillations in molecular clouds

In Papers I & II we demonstrated that the simple model of the preceding section is bistable for all values of $Y_{\rm O}^{\rm T}$ and that these solutions can persist in more realistic molecular cloud chemical models. We now show that this is also the case for chemical oscillations. Figure 4.2 shows the chemical evolution for the reference dense cloud model at $n_{\rm H} = 1 \times 10^4$ cm^{-3} and two values of $D_{\rm gr}$. We find that slightly higher values of $T_{\rm gr}$ are required for oscillations to appear than in the pure oxygen chemistry because the presence of other elements (C,N,S) can shift the range of $\zeta/n_{\rm H}$ for bistability to higher $n_{\rm H}$ (Paper I).

4.5.1 Relaxation oscillations at $\mathbf{n}_H = 1{\times}10^4$ cm^{-3}

Figure 4.2(a) shows that nonlinear relaxation oscillations are present for $T_{\rm gr} = 15.26$K. The time series of the abundance oscillations are different from those found in §4.4 and are generally characterised by a 'ringdown' of decaying amplitude and increasing period. Gaseous O, O_2, N and N_2 are regulated by thermal desorption and the amplitude of the oscillations corresponds to variations of $\sim 10^2 - 10^3$ in the OH, O_2 and H_2O abundances. NH_3 can oscillate in abundance by a factor of $\sim 10^5$. The nitrogen chemistry is coupled to that of oxygen through the reaction sequence that catalyses N_2 formation in molecular clouds

$$\mathrm{N} \xrightarrow{\mathrm{OH}} \mathrm{NO} \xrightarrow{\mathrm{N}} \mathrm{N_2} + \mathrm{O}. \tag{4.9}$$

An important point is that the nitrogen chemistry does not directly affect the oxygen chemistry: no oxygen is directly lost in the sequence (4.9) and the reaction

$$\mathrm{N} + \mathrm{O_2} \longrightarrow \mathrm{NO} + \mathrm{O} \tag{4.10}$$

has a negligible rate at low temperatures (e.g. McElroy et al. (2013)). As noted in §4.2.2, CO formation through

$$\mathrm{C} + \mathrm{OH} \longrightarrow \mathrm{CO} + \mathrm{H} \tag{4.11}$$

$$\mathrm{C} + \mathrm{O_2} \longrightarrow \mathrm{CO} + \mathrm{O} \tag{4.12}$$

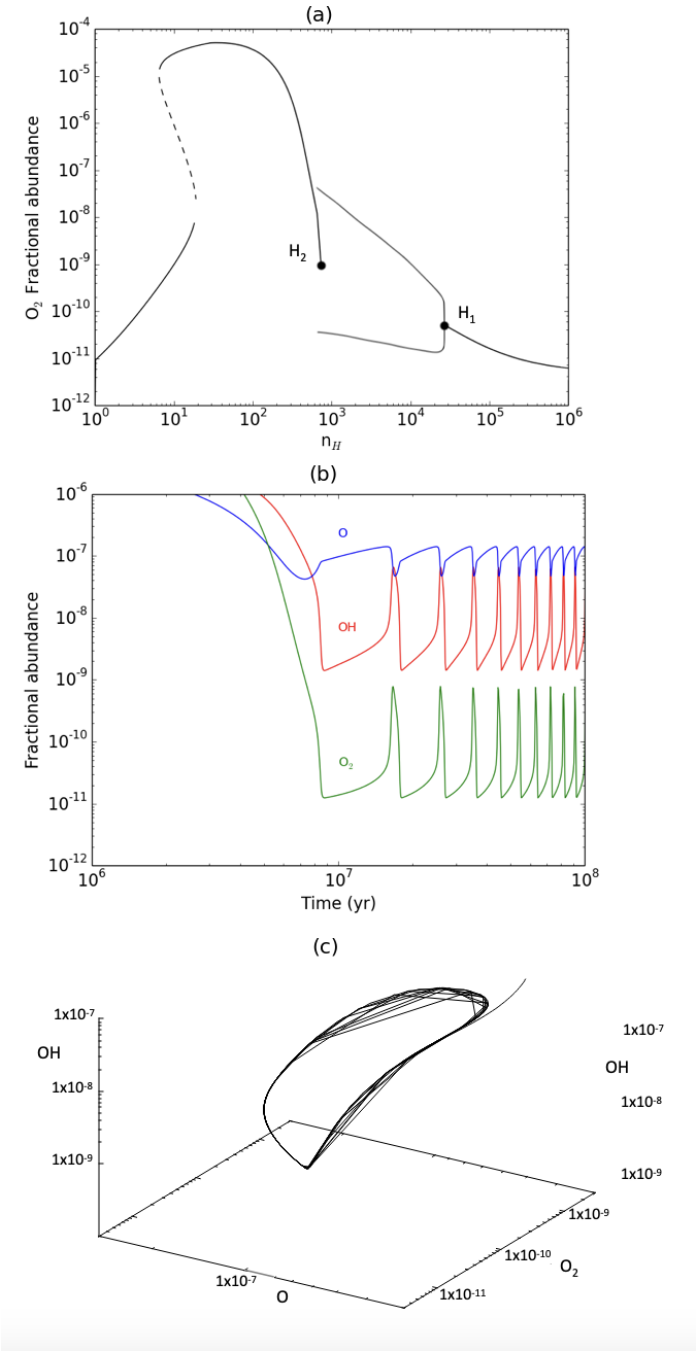

Figure 4.1: (a) Bifurcation diagram for the O_2 abundance in the reduced model for $T_{\rm gr}$ = 14.70K; H_1 and H_2 denote the Hopf bifurcation points; (b) Time series for $y_{\rm O}(t)$, $y_{\rm OH}(t)$ and $y_{\rm O_2}(t)$ at $n_{\rm H} = 1 \times 10^4$ cm^{-3} in the bifurcation diagram; (c) Phase space evolution of the time series of (b);

substantially depletes atomic carbon from the gas within an accretion timescale. This has the effect that, at $T_{\rm gr} \approx 15$K, almost all the carbon in CO is frozen out. Other carbon-bearing molecules also freeze out, as do the sulfur-bearing species. Although the adopted binding energy of atomic S is comparable to that of O_2 (Table 1), it is converted in gas-phase reactions to species with higher binding energies: SO, SO_2 and CS, which do freeze out efficiently.

Our conservative choice of dust parameters (Table 1) and the gas density leads to the nonlinear oscillations appearing, as in the H-He-O model, on timescales ($\gtrsim 10^7$ years) that exceed estimated molecular cloud lifetimes. We note that some estimates of Milky Way GMC lifetimes ($\sim 1.5 - 4 \times 10^7$ years) are in range where chemical oscillations could arise. Figure 4.2(b) shows the chemical evolution in a model with $D_{\rm gr} = 5D^0_{\rm gr}$ and $T_{\rm gr} = 15.46K$. With a slight increase of $T_{\rm gr}$ and a larger dust cross-section, the oscillations can be made to begin at earlier times ($\gtrsim 4 \times 10^6$ years), but with a lower maximum amplitude than in 2(a). Solutions with larger amplitude oscillations should also exist but are difficult to find without a bifurcation diagram for the system; we return to this point in §4.6.

The presence of the relaxation oscillations is a characteristic of a nonlinear dynamical system that has undergone Hopf bifurcation but in which some of the bifurcation parameters vary slowly in time (e.g. Seydel (2009)). In this model the combination of bifurcation parameters $[\zeta/n_{\rm H}; \lambda_k/\xi_k, k = {\rm O}, {\rm O}_2]$ are fixed (at given $T_{\rm gr}$) and, to first order, determine the appearance of the Hopf bifurcation (recall that these also initially fix $Y_{\rm O}$). However, chemical reactions convert O, N and C nuclei in the gas into molecules that can be permanently removed by accretion, depending on $T_{\rm gr}$. This means that the gaseous elemental abundances $Y_{\rm O}(t)$, $Y_{\rm N}(t)$ and $Y_{\rm C}(t)$ undergo a slow quasi-stationary drift in time; even very small changes can have dramatic effects on the evolution. Specifically, $Y_{\rm N}(t)$ declines due to loss of N nuclei in NH_3, NH_2, NH and NO; this affects the oxygen chemistry though the sequence (4.9) and by the direct removal of O nuclei by NO accretion. The slow conversion of the trace amounts of atomic C to CO in reactions (4.11) and (4.12), followed by CO accretion, also influences $Y_{\rm O}(t)$ and $Y_{\rm C}(t)$.

4.5.2 Relaxation oscillations at $\mathbf{n}_H = 1{\times}10^5$ cm^{-3}

The models of Figure 4.2 show no evidence for chaotic dynamics. These chemical models are similar in composition to observed cloud cores in which gaseous CO has a low abundance, disappearing at the highest densities while those of N_2 (N_2H^+) and NH_3 can still be present (e.g. Bergin & Tafalla (2007); Wirström et al. (2012); Sipilä et al. (2019)). Such CO-depleted cores typically have $\sim 10 - 100$ times greater densities and so we next consider a higher density model.

Adopting $n_{\rm H} = 1 \times 10^5$ cm^{-3}, we also set $\zeta = 10\zeta_0$ to maintain the same $\zeta/n_{\rm H}$ ratio so that a gas-phase bistable solution can approximately be recovered. As before, slightly higher $T_{\rm gr}$ values are required for oscillations to occur. Figure 4.3 shows the time series for the long-term evolution of selected species as a function of $T_{\rm gr}$ and that

relaxation oscillations now begin after one accretion time ($\gtrsim 10^6$ years), a time-scale that is relevant for comparison with molecular cloud chemistry.

4.6 Discussion

The gas-grain models considered here, evolve to produce the conditions of CO-depleted dense cores (e.g. Bergin & Tafalla (2007)). When the mechanism mediating the gas-grain exchange of molecules is thermal desorption, grain temperatures of $T_{\rm gr} \gtrsim$ 20K would be required for the models to maintain significant CO abundances at later times. The C and C^+ released from CO could then influence the O_2-O autocatalysis and the nonlinear solutions found here (§4.5, Paper I). Furthermore, alternatives to the UMIST $E_{\rm B}$ values of Table 1 exist[2] experimental measurements of $E_{\rm B}$ for O atom binding on water ice lie in the range 1440 − 1660K (He et al. (2015); Minissale et al. (2022)). Thus, to produce oscillations in these models via O_2-O desorption requires higher dust temperatures to match the desorption rates considered here; $\xi_{\rm O}(T_{\rm gr})$ and $\xi_{\rm O_2}(T_{\rm gr})$ at 15K requires $T_{\rm gr} \approx 27 - 31$K. However, while $T_{\rm gr}$ in this range will also desorb CO and other molecules, making the chemistry similar to that of dense clouds, the $\zeta/n_{\rm H}$ range for bistability in the gas will be different due to the presence of the additional elements, particularly C and S (Paper I) and so a search of the parameter space for Hopf bifurcations would be required.

In fact, other autocatalytic cycles and bistable solutions are present in interstellar chemistry (Paper II) and these could also be made to undergo Hopf bifurcation. Atomic nitrogen can act as an autocatalyst and bistable states appear at densities of $\sim 10^5$ cm^{-3} and higher, for all values of $Y_{\rm N}^{\rm T}$. Although we did not consider grain-surface chemistry explicitly, we note that estimates of the binding energies of CH_n with n=1,3; species are low enough (Penteado et al. (2017); Wakelam et al. (2017a)) that they could be desorbed, along with CH_4, either thermally or by reactive desorption (e.g. Brown & Charnley (1990)). As gas-phase carbon chemistry has an autocatalytic cycle, nonlinear oscillations could then be generated by gas-dust exchange of the methylidyne radical autocatalyst (CH).

Other desorption mechanisms are possible, including non-thermal desorption and reactive desorption (e.g. Leger et al. (1985); Minissale et al. (2016b); Chuang et al. (2018); Sipilä et al. (2021); Wakelam et al. (2021)). As long as the rates of any alternative desorption mechanism returns O and O_2 at the same rates as those considered here oscillations should still occur, i.e. for non-thermal desorption $\xi_{\rm NT} \sim \xi_{\rm O}\ (T_{\rm gr}) \approx 15$K). Our assumption that $T = T_{\rm gr}$ is consistent with thermal balance in dense clouds but is not necessarily applicable when non-thermal desorption is considered. However, we find that models in which this condition is relaxed ($T \neq T_{\rm gr}$) produce similar dynamical solutions. Reactive desorption of grain-surface reaction products could, in principle, still produce oscillations if the sum of the their desorption rates, and the

[2]See Minissale et al. (2022) for a recent review of the physics of thermal desorption relevant to interstellar dust.

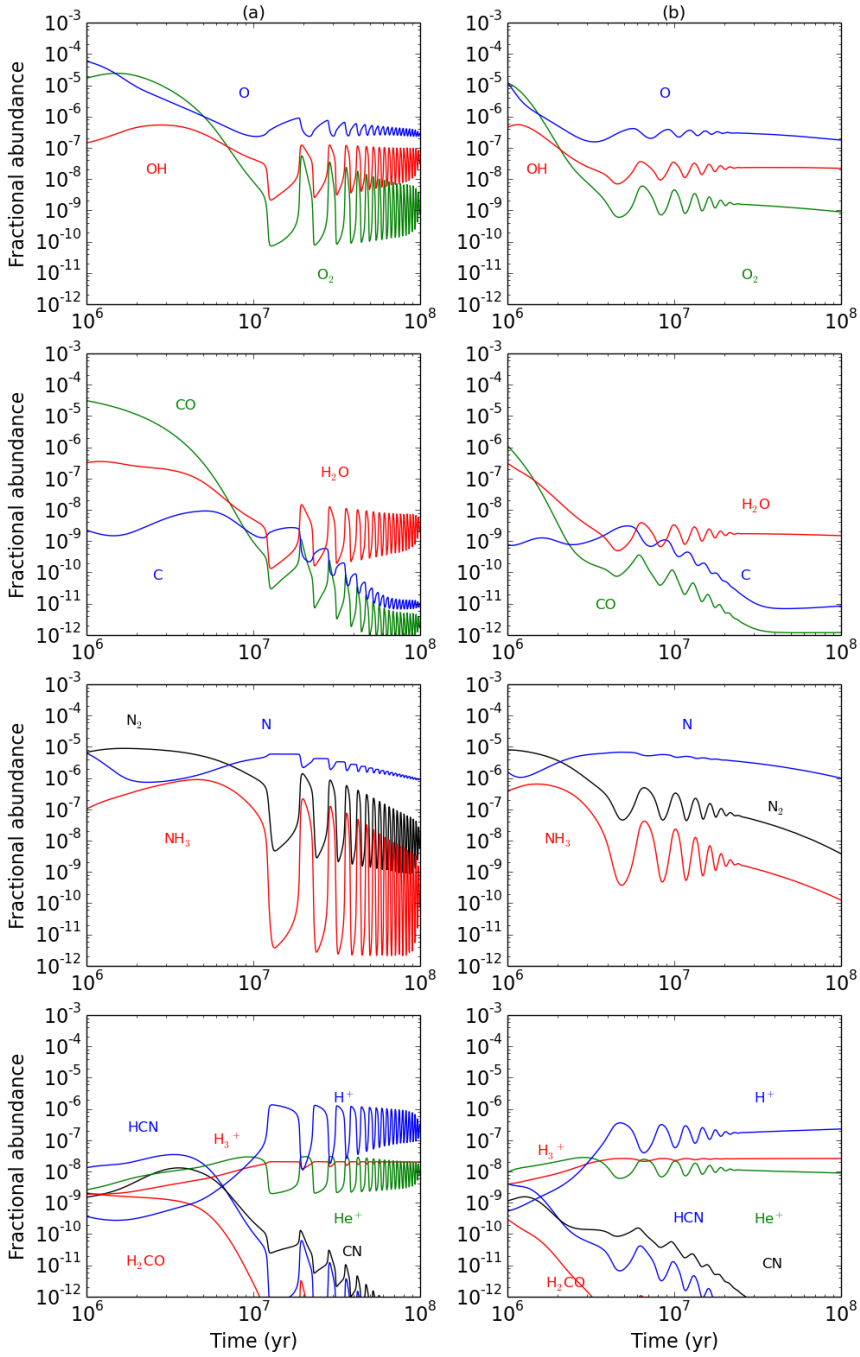

Figure 4.2: Gas-grain chemical evolution in a dense molecular cloud for $\zeta = \zeta_0$ and $n_{\rm H} = 1 \times 10^4$ cm^{-3}: (a) Left-hand panels, $D_{\rm gr} = D^0_{\rm gr}$, $T_{\rm gr} = 15.26K$; (b) Right-hand panels $D_{\rm gr} = 5D^0_{\rm gr}$, $T_{\rm gr} = 15.46$K.

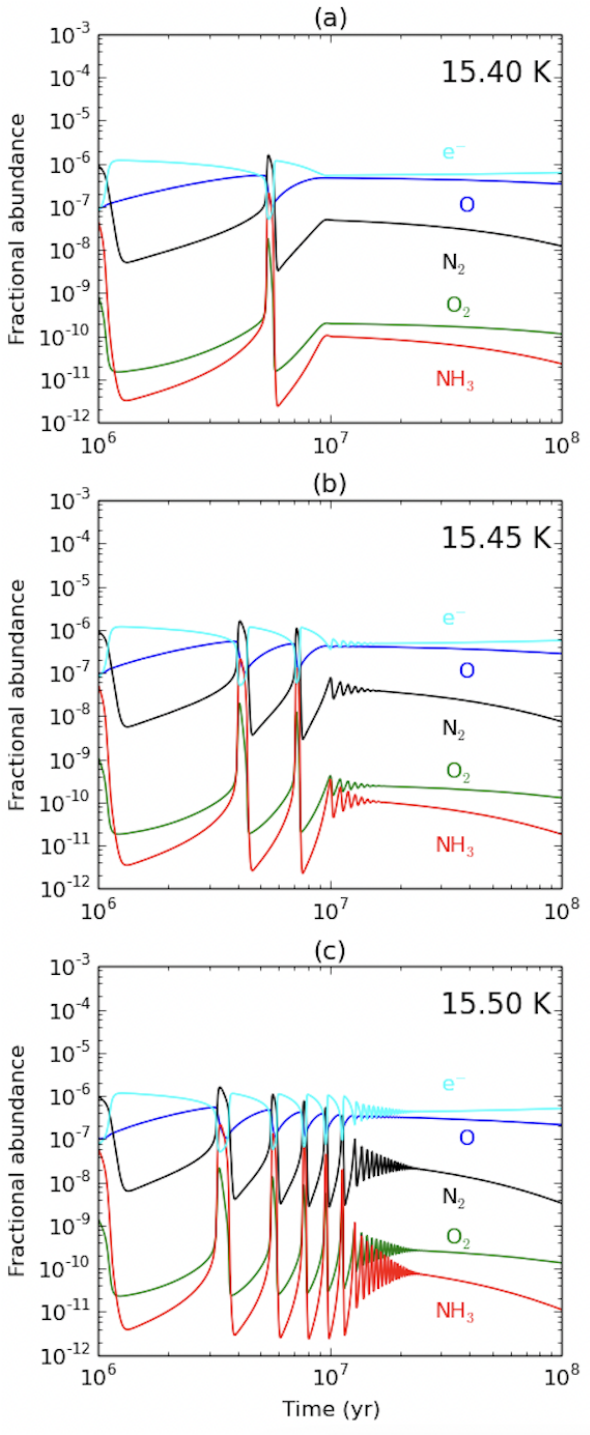

Figure 4.3: Gas-grain chemical evolution of selected species as a function of the bifurcation parameter $T_{\rm gr}$. This model has $\zeta = 10\zeta_0$, $n_{\rm H} = 1 \times 10^5$ cm^{-3}, $D_{\rm gr} = D_{\rm gr}^0$ and the $T_{\rm gr}$ are given in the upper right-hand corner of each panel.

rate of their subsequent breakdown in gas-phase reactions to an X_2-X pair, matches the thermal desorption rates found here.

Finally, the above brings us to the important point that searching for oscillations without bifurcation diagrams (i.e. employing ODEs or scaling from known solutions) is risky. Their appearance depends sensitively on the bifurcation parameters, $\zeta/n_{\rm H}$ and λ_k/ξ_k, which are are coupled through $n_{\rm H}$ and T (when $T = T_{\rm gr}$ is assumed), and the relative elemental abundances. To find Hopf bifurcations and oscillations would first require a bifurcation analysis of the full CHONS gas-phase chemistry to locate the range of $\zeta/n_{\rm H}$ and elemental abundances to produce bistable solutions (Dufour & Charnley 2022). This can then be followed by mathematical analysis of the stability of the solutions for the gas-grain chemistry (Gray & Scott (1996)). Analysis of this model from the perspective of the non-linear dynamics is beyond the scope of this article and will be considered elsewhere.

4.7 Conclusions

Autocatalysis in interstellar gas-phase chemistry can lead to bistability which, when coupled with the gas-grain exchange of key species, can undergo Hopf bifurcation and lead to the appearance of limit cycles, chemical relaxation oscillations. The non-linear oscillations in these models occur on time-scales relevant for comparison with molecular cloud composition, particularly the first few periods.

These results complement the limit cycle oscillations recently presented by Roueff & Le Bourlot (2020). Both these studies indicate the early-time/late-time dichotomy of molecular cloud modeling can be broken, and predict dramatically different chemical evolution from that found heretofore. The chemical processes that determine the oscillatory solutions are central to almost all chemical models of astrophysical sources, including interstellar clouds and protoplanetary disks. Oscillations are therefore fundamental outcomes in astrochemical kinetics, indicating that a wealth of non-linear dynamical phenomena can be present in cold molecular clouds.